Supplemental Materials

Molecular Biology of the Cell

Zhang *et al*.

Figure 1–figure supplement 1. DNA damage-induced APBs exhibit liquid behavior and enrich SUMO2/3. (A) Dependence of fusion time on fusion length, defined as the length of the long axis of the object when two droplets start fusing. Each point represents one fusion event. The black line is a linear fit with a slope of 54 s/μm. (B) Immunofluorescence images of SUMO2/3 for cells with FokI or a nuclease dead FokI mutant targeted to telomeres. The overlay of FokI (purple) and SUMO2/3 (green) appears white (B). Graphs show the percent of telomeres with SUMO2/3 foci (C) and the integrated intensity of SUMO2/3 foci on telomeres (D). Each data point represents one cell, black lines mean, gray bars 95% confidence interval. Scale bars 5 μm.

Figure 2–figure supplement 1. SUMO1 is enriched on telomeres after SIM recruitment. Immunofluorescence images of SUMO1 after recruiting SIM or SIM mutant to telomeres (A), and quantification of the number of telomeres with SUMO1 foci per cell (B) and the integrated intensity of SUMO1 foci on telomeres per cell (C). Each data point in (B) and (C) represents one cell from two biological replicates, black line represents the average value, and gray bar represents 95% confidence interval. Scale bars 5 μm.

Figure 3–figure supplement 1. Liquid behavior of SIM dimerization-induced condensates. (A) Dependence of fusion time on fusion length for SIM dimerization. Each point represents one fusion event. The black line is a linear fit with a slope of 29 s/μm. (B-E) 5% 1,6-hexanediaol (B, C, 36 cells from three duplicates) or 0.6 M NaCl (D, E, 22 cells from two duplicates) was added to U2OS cells after 3 hours of dimerizing SIM with TNH. Graphs show mean integrated intensity in TRF1 and SIM foci over time (error bars, SEM). (F, G) Representative images and percent of intensity loss (G) in foci after adding different amount of NaCl (>9 cells for each condition, error bar, STD). Images: insets two times enlarged, scale bars 5 μm.

Figure 3–figure supplement 2. SIM mutant recruited to telomeres cannot induce condensation and clustering. TNH was added to cells expressing SIM mutant-mCherry-DHFR and Halo-GFP-TRF1 after the first time point to induce dimerization. Graphs show mean integrated intensity per TRF1 and SIM mutant foci (B) and number

of TRF1 and SIM mutant foci (C) over time. Error bars STD, 20 cells from two duplicates. In contrast to SIM recruitment, telomere number stayed unchanged and the intensity was not increased, but decreased due to photobleaching. P value between first and last time point for TRF1 foci intensity < 0.001, SIM foci intensity < 0.001, TRF1 foci number < 0.001 and SIM foci number < 0.001. Scale bars 5 μm.

Figure 4–figure supplement 1. Unlike damaged-induced APBs, dimerization-induced condensates do not enrich 53BP1 or POLD3. 53BP1 (A-C) or POLD3 (D-F) immunofluorescence after FokI tethering or SIM recruitment to telomeres. Images: insets two times enlarged, scale bars 5 μm. Graphs show number and integrated intensity of 53BP1 (B, C) or POLD3 (E, F) foci per cell colocalized with FokI or SIM.

Figure 4–figure supplement 2. PCNA fused to SUMO1 is enriched in SIM dimerization-induced condensates. (A) Images of GFP-PCNA-SUMO1 and mCherry-eDHFR-SIM (or SIM mutant) 2 hours after adding TNH, using Halo-TRF1 as an anchor for dimerization in U2OS cells. Insets two times enlarged, scale bars 5 μm. Graphs show number (B) and integrated intensity (C) of PCNA-SUMO1 foci per cell colocalized with SIM or SIM mutant.

Figure 4–figure supplement 3. Dimerization-induced telomere clustering does not result in nascent telomere DNA synthesis. (A) Images of EdU following FokI tethering or SIM or SIM mutant recruitment in non-S phase U2OS cells (insets two times enlarged, scale bars 5 μm). S-phase cells, identified based on high and cell-wide EdU signal, were excluded from the analysis. Graphs show number (B) and integrated intensity (C) of EdU foci per cell colocalized with FokI, SIM, or SIM mutant.

Figure1-S1

(A)

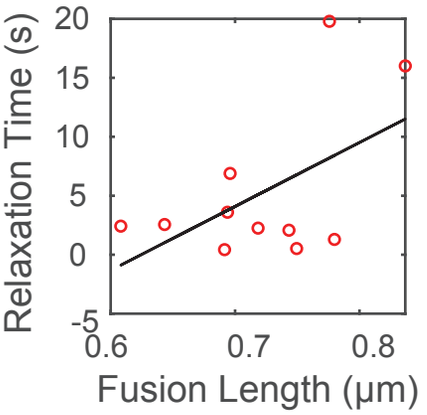

(B)

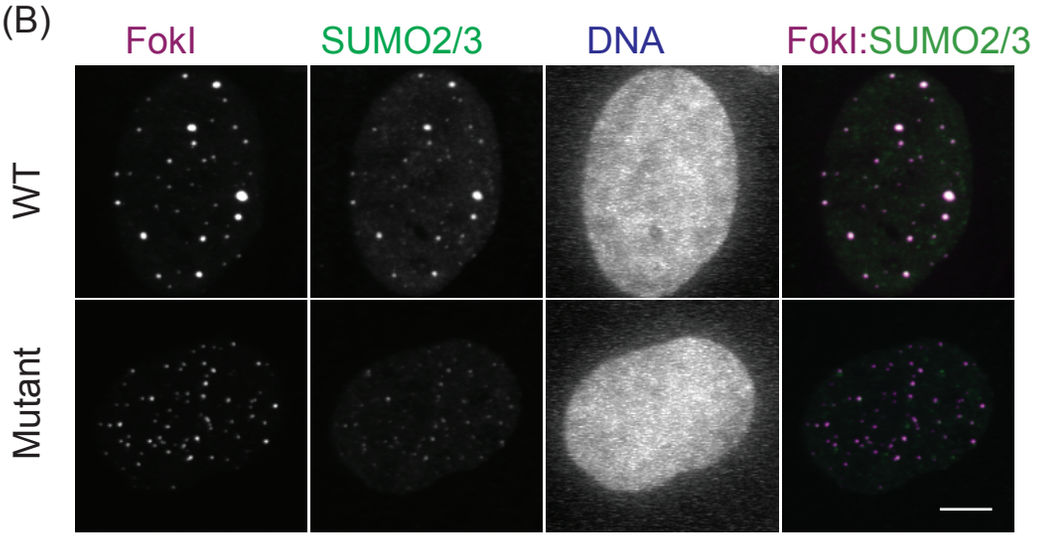

(C)

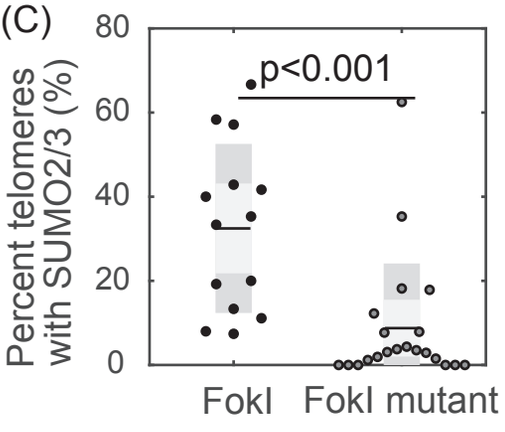

(D)

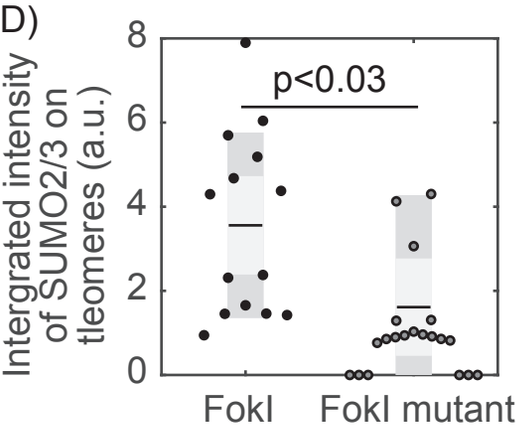

Figure 2-S1

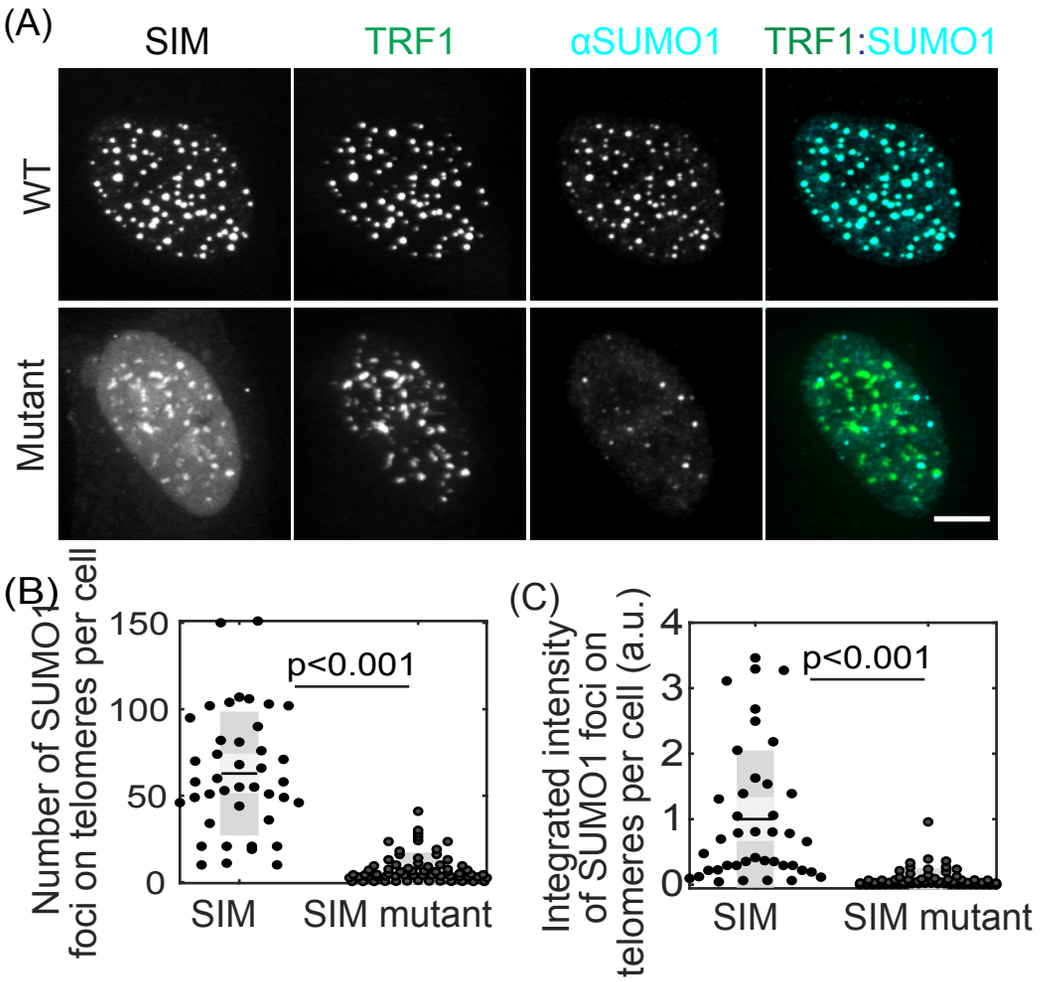
(A)
SIM
TRF1
αSUMO1
TRF1:SUMO1
WT
Mutant
(B)
Number of SUMO1 foci on telomeres per cell
150
100
50
0
p<0.001
SIM
SIM mutant
(C)
Integrated intensity of SUMO1 foci on telomeres per cell (a.u.)
4
3
2
1
0
p<0.001
SIM
SIM mutant

Figure 3-S1

(A)

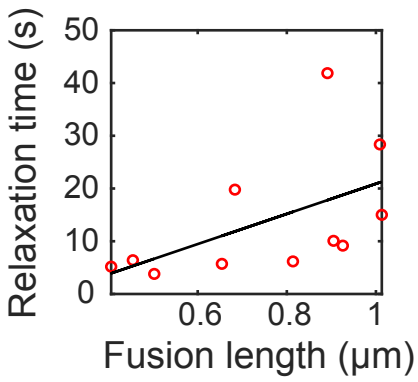

(G)

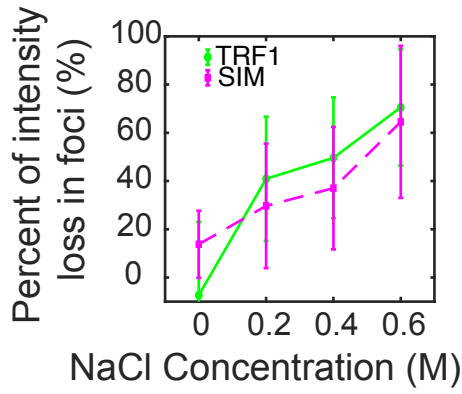

Add 1,6-hexanediol

(B)

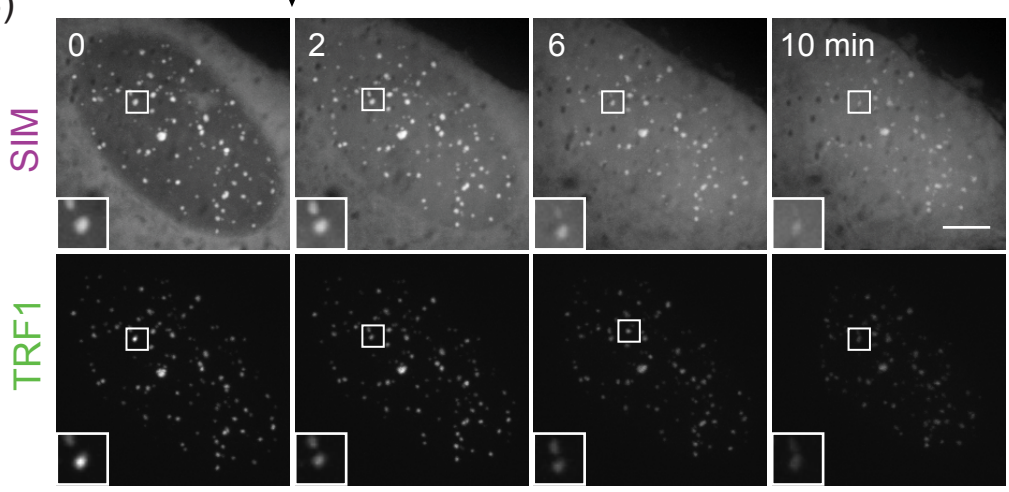

(C)

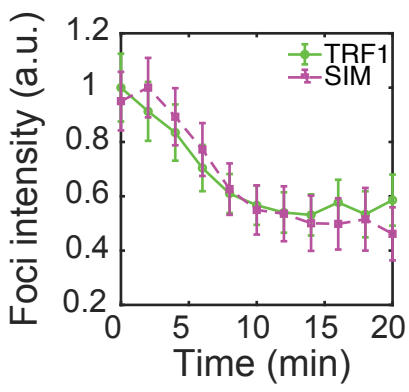

(E)

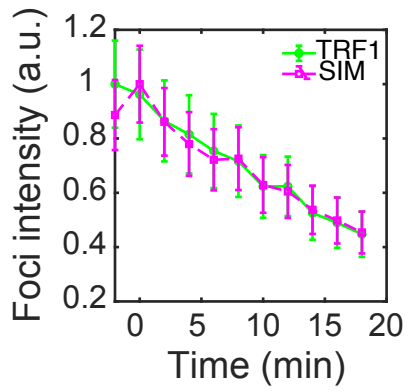

Add NaCl

(D)

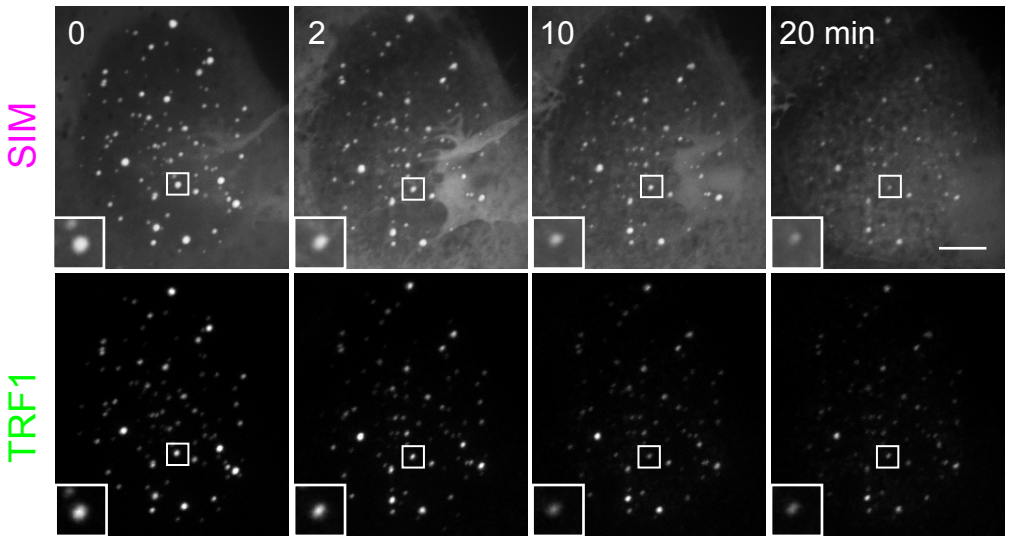

(F)

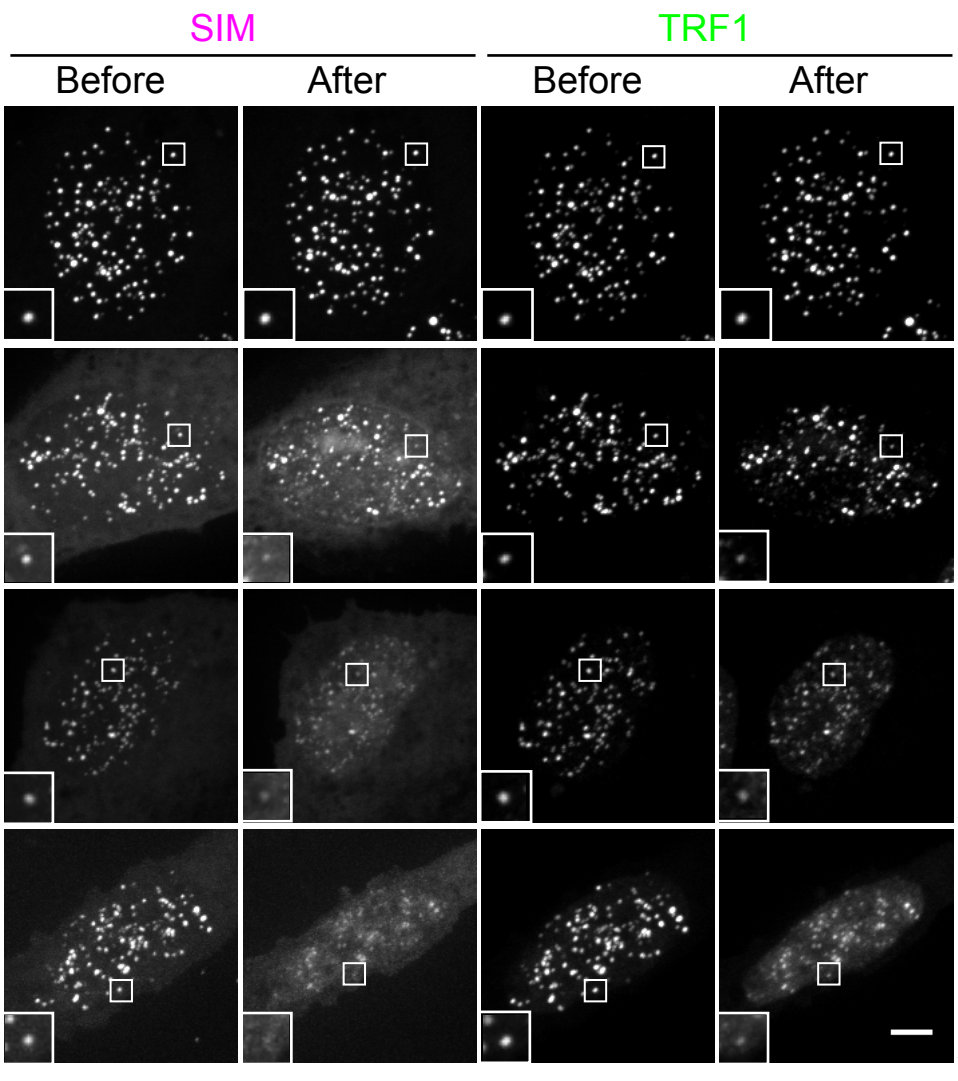

Figure 3-S2

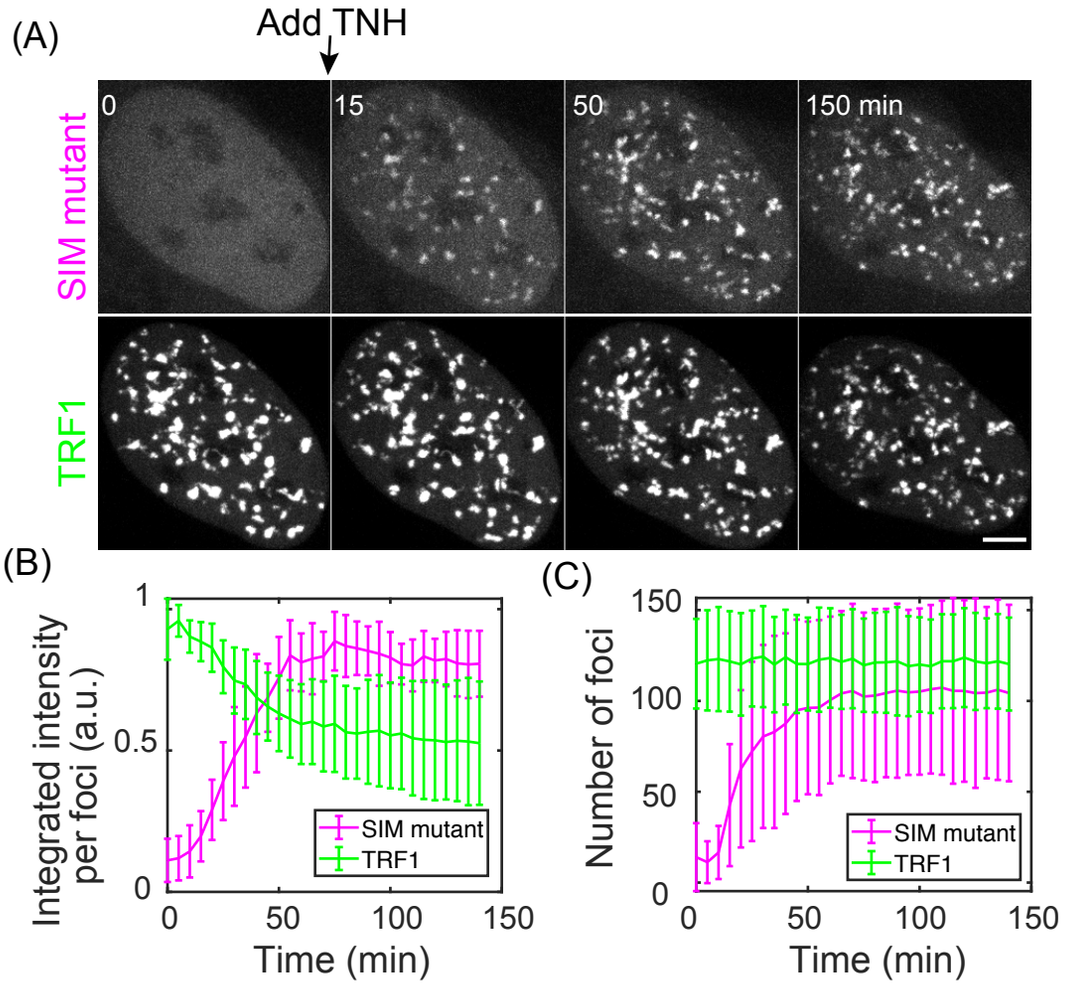
(A)
Add TNH
SIM mutant
TRF1
0
15
50
150 min
(B)
Integrated intensity per foci (a.u.)
1
0.5
0
0
50
100
150
Time (min)
SIM mutant
TRF1
(C)
Number of foci
150
100
50
0
0
50
100
150
Time (min)
SIM mutant
TRF1

Figure 4-S1

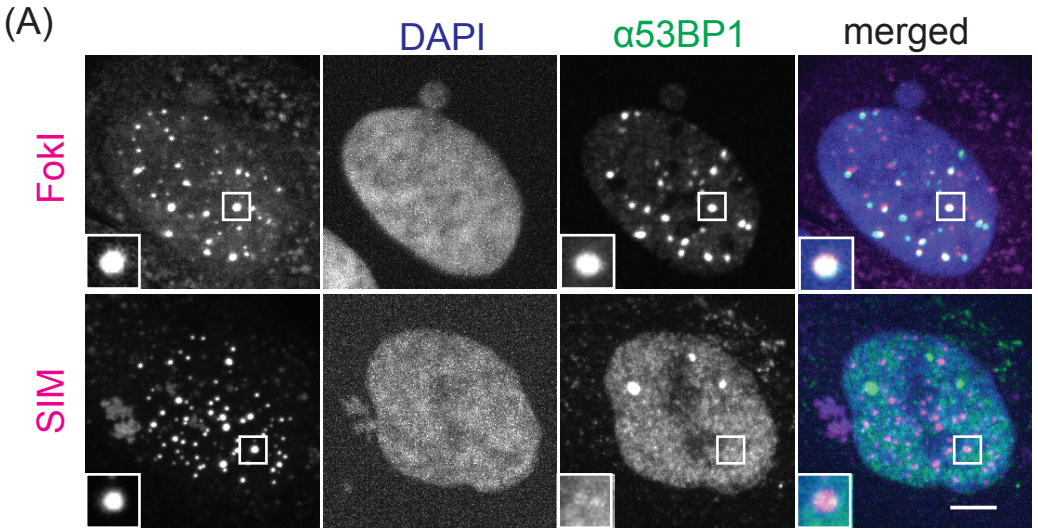
(A)
DAPI
α53BP1
merged
FokI
SIM

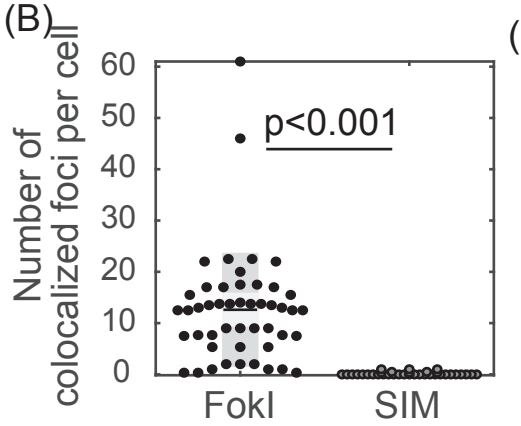
(B)
Number of colocalized foci per cell
60
50
40
30
20
10
0
p<0.001
FokI
SIM

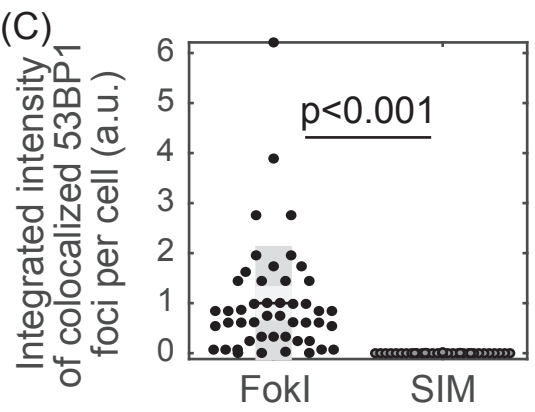
(C)
Integrated intensity of colocalized 53BP1 foci per cell (a.u.)
6
5
4
3
2
1
0
p<0.001
FokI
SIM

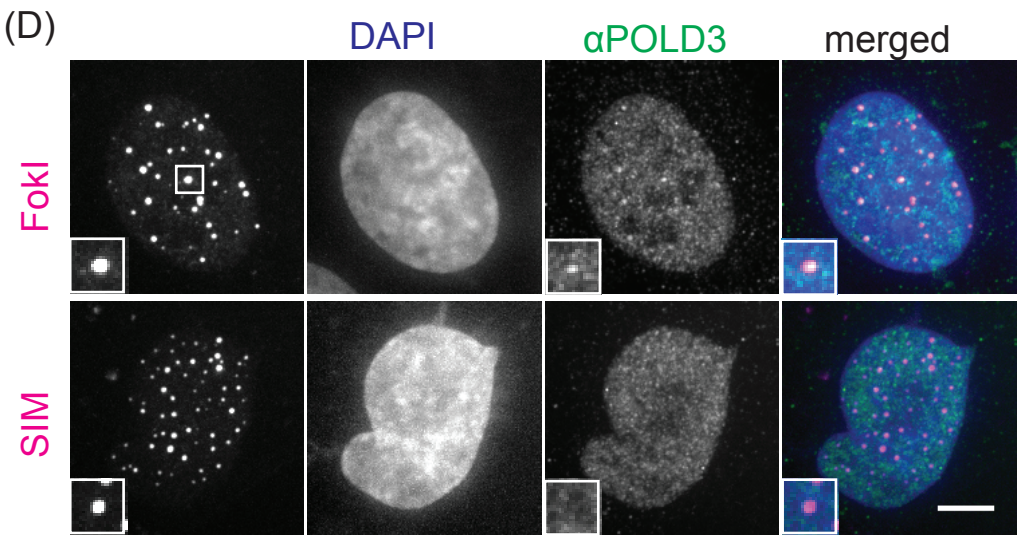
(D)
DAPI
αPOLD3
merged
FokI
SIM

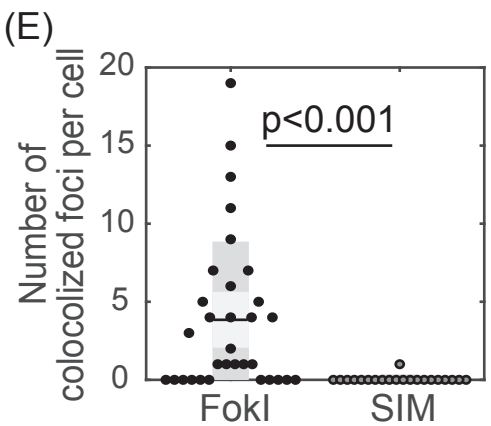
(E)
Number of colocolized foci per cell
20
15
10
5
0
p<0.001
FokI
SIM

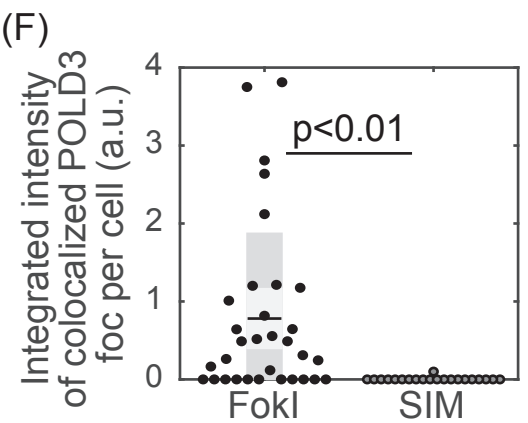
(F)
Integrated intensity of colocalized POLD3 foc per cell (a.u.)
4
3
2
1
0
p<0.01
FokI
SIM

Figure 4-S2

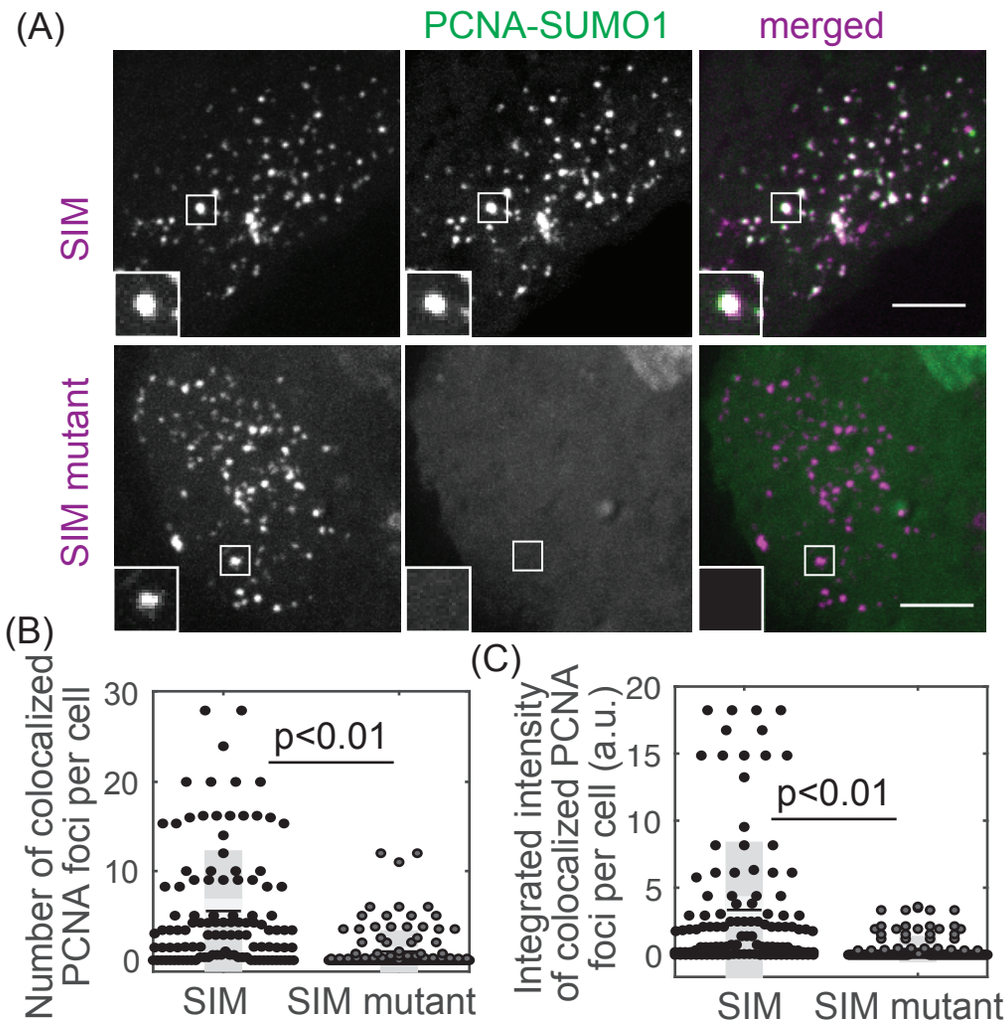
(A)
PCNA-SUMO1
merged
SIM
SIM mutant

(B)
Number of colocalized PCNA foci per cell
30
20
10
0
p<0.01
SIM
SIM mutant

(C)
Integrated intensity of colocalized PCNA foci per cell (a.u.)
20
15
10
5
0
p<0.01
SIM
SIM mutant

Figure 4-S3.

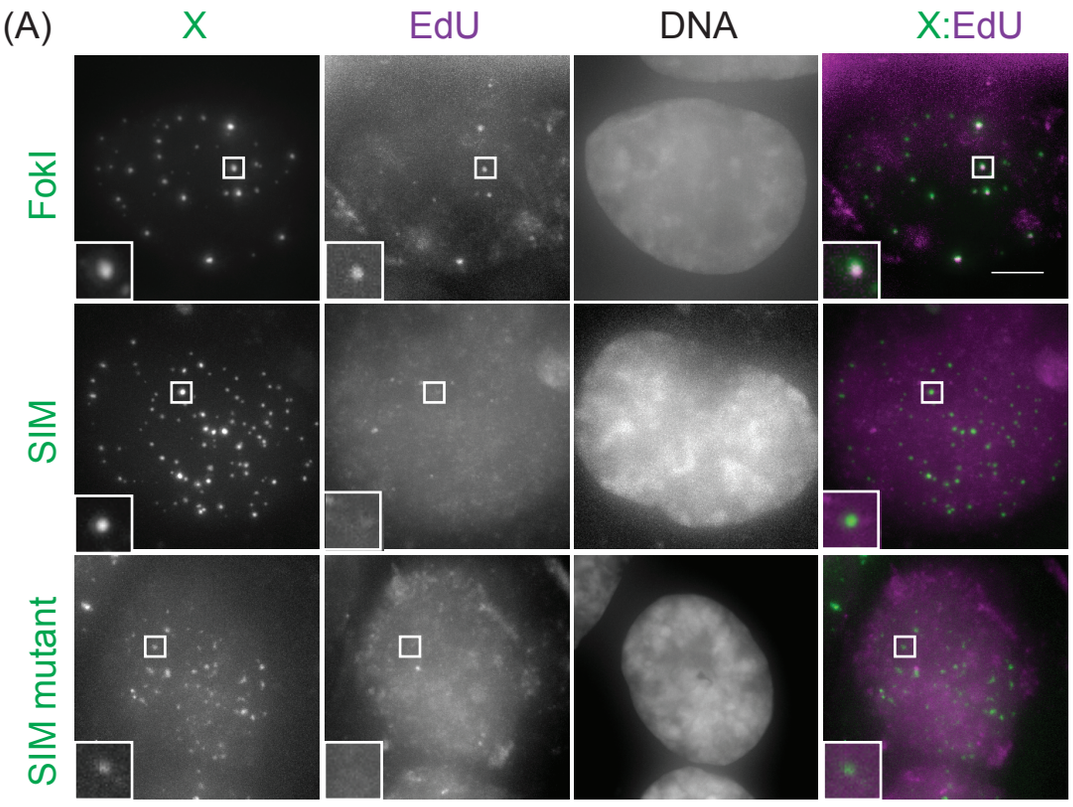
(A)
X
EdU
DNA
X:EdU
FokI
SIM
SIM mutant

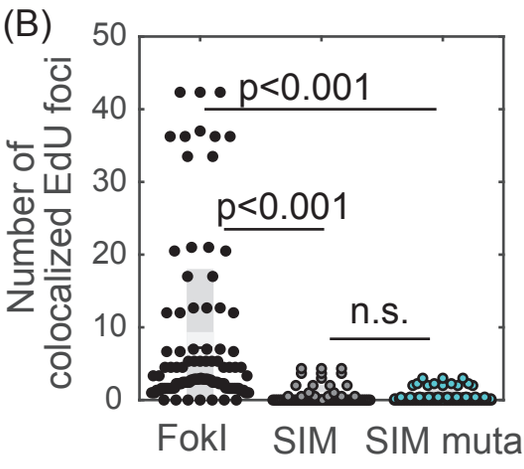
(B)
Number of colocalized EdU foci
50
40
30
20
10
0
p<0.001
p<0.001
n.s.
FokI
SIM
SIM mutant

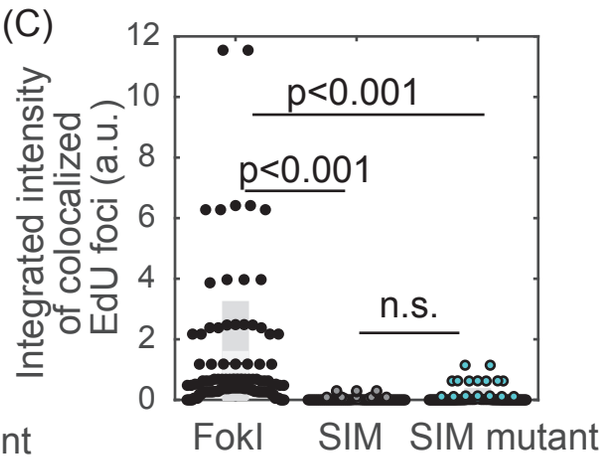
(C)
Integrated intensity of colocalized EdU foci (a.u.)
12
10
8
6
4
2
0
p<0.001
p<0.001
n.s.
FokI
SIM
SIM mutant

Table 1 List of APB components that contain sumoylation sites or SIMs

APB component	# of Sumoylation sites	# of SIMs
Rpa	2(ref 1)	
Rad50/Mre11/NBS1 complex	3(ref 2)	2(ref 3)
WRN	1(ref 4)	
BRCA1	2(ref 5)	1(ref 5)
XRCC3	1(ref 6)	1(ref 7)
pRb	1(ref 8)	
STN1		1(ref 9)
TPZ1	1(ref 10)	
53BP1	1(ref 11)	
Rif1	1(ref 12)	
hnRNP A2	1(ref 13)	
HP1 α, β, γ	1(ref 14)	
ATM	1(ref 15)	
ATR	1(ref 15)	
CDK2		1(ref 16)
FANCA, FANCD2	1(ref 17)	1(ref 18)
SLX4	1(ref 19)	1(ref 19)
FEN1	4(ref 20)	
γ-H2AX	2(ref 21)	
Hsp90	1(ref 22)	

MDC1	1(ref 23)	
MUS81	2(ref 24)	
NXP2	5(ref 25)	1(ref 25)
PARP1	2(ref 26)	
POT1	1(ref 27)	
Rad51	1(ref 28)	1(ref 28)
Rad52	1(ref 29)	1(ref 29)
BLM	3(ref 30)	2(ref 30)
SMC5/6	1(ref 31)	
TopoIIα	1(ref 32)	
PML	3(ref 33)	1(ref 33)
P53	1(ref 34)	
SP100	1(ref 35)	1(ref 36)
Daxx	2(ref 37)	1(ref 38)
RAP1	1(ref 39)	
TRF1, TRF2,	1(ref 40)	
PCNA	2(ref 29)	1(ref 29)

References

1. Dou H, Huang C, Singh M, Carpenter PB, Yeh ET. Regulation of DNA repair through deSUMOylation and SUMOylation of replication protein A complex. Mol Cell. 2010;39(3):333–345. doi:10.1016/j.molcel.2010.07.021
2. Sohn SY, Hearing P. Adenovirus regulates sumoylation of Mre11-Rad50-Nbs1 components through a paralog-specific mechanism. J Virol. 2012;86(18):9656–9665. doi:10.1128/JVI.01273-12

3. Chen YJ, Chuang YC, Chuang CN, et al. S. cerevisiae Mre11 recruits conjugated SUMO moieties to facilitate the assembly and function of the Mre11-Rad50-Xrs2 complex. Nucleic Acids Res. 2016;44(5):2199–2213. doi:10.1093/nar/gkv1523
4. Kawabe, Y. et al. Covalent modification of the Werner's syndrome gene product with the ubiquitin-related protein, SUMO-1. J. Biol. Chem. 275, 20963–20966 (2000).
5. Aurélie Vialter, Anne Vincent, Aïcha Demidem, Daniel Morvan, Georges Stepien, Nicole Dalla Venezia, Pascale G. Rio, Cell cycle-dependent conjugation of endogenous BRCA1 protein with SUMO-2/3, Biochimica et Biophysica Acta (BBA) - General Subjects, Volume 1810, Issue 4, 2011, Pages 432-438, ISSN 0304-4165.
6. Ling-Yueh Hu, Che-Chang Chang, Yen-Sung Huang, Wen-Cheng Chou, Ying-Mei Lin, Chun-Chen Ho, Wei-Ting Chen, Hsiu-Ming Shih, Chia-Ni Hsiung, Pei-Ei Wu, Chen-Yang Shen, SUMOylation of XRCC1 activated by poly (ADP-ribosyl)ation regulates DNA repair, Human Molecular Genetics, Volume 27, Issue 13, 01 July 2018, Pages 2306–2317, https://doi.org/10.1093/hmg/ddy135
7. Wiest NE, Tomkinson AE. SUMOning the base excision repair machinery for differentiation. EMBO J. 2019;38(1):e101147. doi:10.15252/embj.2018101147
8. Ledl, A., Schmidt, D. & Müller, S. Viral oncoproteins E1A and E7 and cellular LxCxE proteins repress SUMO modification of the retinoblastoma tumor suppressor. Oncogene 24, 3810–3818 (2005). https://doi.org/10.1038/sj.onc.1208539
9. Matmati, S., Vaurs, M., Escandell, J. M., Maestroni, L., Nakamura, T. M., Ferreira, M. G., … Coulon, S. (2018). The fission yeast Stn1-Ten1 complex limits telomerase activity via its SUMO-interacting motif and promotes telomeres replication. Science Advances, 4(5), eaar2740. https://doi.org/10.1126/sciadv.aar2740
10. Garg M, Gurung RL, Mansoubi S, et al. Tpz1TPP1 SUMOylation reveals evolutionary conservation of SUMO-dependent Stn1 telomere association. EMBO Rep. 2014;15(8):871–877. doi:10.15252/embr.201438919
11. Galanty Y, Belotserkovskaya R, Coates J, Polo S, Miller KM, Jackson SP.

2009Mammalian SUMO E3-ligases PIAS1 and PIAS4 promote responses to DNA double-strand breaks. Nature 462, 935–939.

12. Kumar R, Cheok CF. Dynamics of RIF1 SUMOylation is regulated by PIAS4 in the maintenance of Genomic Stability [published correction appears in Sci Rep. 2018 Mar 22;8(1):5236]. Sci Rep. 2017;7(1):17367. Published 2017 Dec 12. doi:10.1038/s41598-017-16934-w
13. Vassileva MT, Matunis MJ. SUMO modification of heterogeneous nuclear ribonucleoproteins. Mol Cell Biol. 2004;24(9):3623–3632. doi:10.1128/mcb.24.9.3623-3632.2004
14. Maison C, Quivy JP, Almouzni G. Suv39h1 links the SUMO pathway to constitutive heterochromatin. Mol Cell Oncol. 2016;3(6):e1225546. Published 2016 Aug 26. doi:10.1080/23723556.2016.1225546
15. Stephanie Munk, Jón Otti Sigurðsson, Zhenyu Xiao, Tanveer Singh Batth, Giulia Franciosa, Louise von Stechow, Andres Joaquin Lopez-Contreras, Alfred Cornelis Otto Vertegaal, Jesper Velgaard Olsen, Proteomics Reveals Global Regulation of Protein SUMOylation by ATM and ATR Kinases during Replication Stress, Cell Reports, Volume 21, Issue 2, 2017, Pages 546-558, ISSN 2211-1247,
16. Meng F, Qian J, Yue H, Li X, Xue K. SUMOylation of Rb enhances its binding with CDK2 and phosphorylation at early G1 phase. Cell Cycle. 2016;15(13):1724–1732. doi:10.1080/15384101.2016.1182267
17. Coleman KE, Huang TT. How SUMOylation Fine-Tunes the Fanconi Anemia DNA Repair Pathway. Front Genet. 2016;7:61. Published 2016 Apr 19. doi:10.3389/fgene.2016.00061
18. Yang K, Moldovan GL, Vinciguerra P, Murai J, Takeda S, D'Andrea AD. Regulation of the Fanconi anemia pathway by a SUMO-like delivery network. Genes Dev. 2011;25(17):1847–1858. doi:10.1101/gad.17020911
19. Yalçin Zeliha, Selenz Carolin, Jacobs Jacqueline J. L. Ubiquitination and SUMOylation in Telomere Maintenance and Dysfunction Frontiers in Genetics 8 2017 10.3389/fgene.2017.00067

20. Yal√ßin Zeliha, Selenz Carolin, Jacobs Jacqueline J. L. Ubiquitination and SUMOylation in Telomere Maintenance and Dysfunction Frontiers in Genetics 8 2017 10.3389/fgene.2017.00067
21. Chen WT, Alpert A, Leiter C, Gong F, Jackson SP, Miller KM. Systematic identification of functional residues in mammalian histone H2AX. Mol Cell Biol. 2013;33(1):111–126. doi:10.1128/MCB.01024-12
22. Wolmarans, A., Kwantes, A., & LaPointe, P. (2019). A novel method for site-specific chemical SUMOylation: SUMOylation of Hsp90 modulates co-chaperone binding in vitro, Biological Chemistry, 400(4), 487-500. doi: https://doi.org/10.1515/hsz-2018-0251
23. Luo K, Zhang H, Wang L, Yuan J, Lou Z. Sumoylation of MDC1 is important for proper DNA damage response. EMBO J. 2012;31(13):3008–3019. doi:10.1038/emboj.2012.158
24. Hu L, Yang F, Lu L, Dai W. Arsenic-induced sumoylation of Mus81 is involved in regulating genomic stability. Cell Cycle. 2017;16(8):802–811. doi:10.1080/15384101.2017.1302628
25. Mimura, Y., Takahashi, K., Kawata, K., Akazawa, T., & Inoue, N. (2010). Two-step colocalization of MORC3 with PML nuclear bodies. Journal of Cell Science, 123(12), 2014 LP – 2024. https://doi.org/10.1242/jcs.063586
26. Zilio N, Williamson CT, Eustermann S, et al. DNA-dependent SUMO modification of PARP-1. DNA Repair (Amst). 2013;12(9):761–773. doi:10.1016/j.dnarep.2013.07.001
27. Umashankar Singh, Varun Maturi, Bengt Westermark, Evidence for multiple forms and modifications of human POT1, DNA Repair, Volume 12, Issue 11, 2013, Pages 876-877, ISSN 1568-7864, https://doi.org/10.1016/j.dnarep.2013.08.014.
28. Shima, H et al. (2013). Activation of the SUMO modification system is required for the accumulation of RAD51 at sites of DNA damage. J Cell Sci 126, 5284–5292.
29. Silva S, Altmannova V, Eckert-Boulet N, et al. SUMOylation of Rad52-Rad59 synergistically change the outcome of mitotic recombination. DNA Repair (Amst). 2016;42:11–25. doi:10.1016/j.dnarep.2016.04.001

30. Min J, Wright WE, Shay JW. Clustered telomeres in phase-separated nuclear condensates engage mitotic DNA synthesis through BLM and RAD52. Genes Dev. 2019;33(13-14):814–827. doi:10.1101/gad.324905.119
31. Varejão N, Ibars E, Lascorz J, Colomina N, Torres-Rosell J, Reverter D. DNA activates the Nse2/Mms21 SUMO E3 ligase in the Smc5/6 complex. EMBO J. 2018;37(12):e98306. doi:10.15252/embj.201798306
32. Ryu H, Furuta M, Kirkpatrick D, Gygi SP, Azuma Y. PIASy-dependent SUMOylation regulates DNA topoisomerase IIalpha activity. J Cell Biol. 2010;191(4):783–794. doi:10.1083/jcb.201004033
33. Sahin, U et al. (2014). Oxidative stress-induced assembly of PML nuclear bodies controls sumoylation of partner proteins. J Cell Biol 204, 931–945.
34. Schmidt, D. & Müller, S. Members of the PIAS family act as SUMO ligases for c-Jun and p53 and repress p53 activity. Proc. Natl Acad. Sci. USA 99, 2872–2877 (2002).
35. Guion L, Bienkowska-Haba M, DiGiuseppe S, Florin L, Sapp M. PML nuclear body-residing proteins sequentially associate with HPV genome after infectious nuclear delivery. PLoS Pathog. 2019;15(2):e1007590. Published 2019 Feb 25. doi:10.1371/journal.ppat.1007590
36. Zheng, Y., Jayappa, K.D., Ao, Z. et al. Noncovalent SUMO-interaction motifs in HIV integrase play important roles in SUMOylation, cofactor binding, and virus replication. Virol J 16, 42 (2019). https://doi.org/10.1186/s12985-019-1134-8
37. Jang, M. S., Ryu, S. W. & Kim, E. Modification of Daxx by small ubiquitin-related modifier-1. Biochem. Biophys. Res. Commun. 295, 495–500 (2002).
38. Che-Chang Chang, Mandar T. Naik, Yen-Sung Huang, Jen-Chong Jeng, Pei-Hsin Liao, Hong-Yi Kuo, Chun-Chen Ho, Yung-Lin Hsieh, Chiou-Hong Lin, Nai-Jia Huang, Nandita M. Naik, Camy C.-H. Kung, Shu-Yu Lin, Ruey-Hwa Chen, Kun-Sang Chang, Tai-Huang Huang, Hsiu-Ming Shih, Structural and Functional Roles of Daxx SIM Phosphorylation in SUMO Paralog-Selective Binding and Apoptosis Modulation, Molecular Cell, Volume 42, Issue 1, 2011, Pages 62-74, ISSN 1097-2765, https://doi.org/10.1016/j.molcel.2011.02.022.
39. Chymkowitch P, Nguéa AP, Aanes H, et al. Sumoylation of Rap1 mediates the

recruitment of TFIID to promote transcription of ribosomal protein genes [published correction appears in Genome Res. 2017 Feb;27(2):334]. Genome Res. 2015;25(6):897–906. doi:10.1101/gr.185793.114

40. Chung, I, Leonhardt, H, and Rippe, K (2011). De novo assembly of a PML nuclear subcompartment occurs through multiple pathways and induces telomere elongation. J Cell Sci 124, 3603–3618.